Fall 12-2020

The Effect of Compaction Temperature and Pressure on Mechanical Properties of 3D Printed Short Glass Fiber Composites

Pushpashree Jain Ajith Kumar Jain
Old Dominion University, pushpasree.jain.a@gmail.com

THE EFFECT OF COMPACTION TEMPERATURE AND PRESSURE ON MECHANICAL PROPERTIES OF 3D PRINTED SHORT GLASS FIBER COMPOSITES

by

Pushpashree Jain Ajith Kumar Jain
B.E. June 2017, MVJ College of Engineering, Visvesvaraya Technological University, India

A Thesis Submitted to the Faculty of
Old Dominion University in Partial Fulfillment of the
Requirements for the Degree of

MASTER OF SCIENCE

MECHANICAL AND AEROSPACE ENGINEERING

OLD DOMINION UNIVERSITY
December 2020

Approved by:

Dr.Oleksandr Kravchanko (Director)

Dr. Krishnand Kaipa (Member)

Dr.Mileta Tomovic (Member)

Dr.Drew Landman (Member)

ABSTRACT

THE EFFECT OF COMPACTION TEMPERATURE AND PRESSURE ON MECHANICAL PROPERTIES OF 3D PRINTED SHORT GLASS FIBER COMPOSITES

Pushpashree Jain Ajith Kumar Jain
Old Dominion University, 2020
Director: Dr. Oleksandr Kravchenko

Among many thermoplastics that are used in engineering, polyamide 6 (nylon 6) is an extremely versatile engineering thermoplastic. Nylon filled with glass fibers has higher mechanical strength and high wear resistance than general purpose nylon. 3D printed composites, based on fused filament modeling, typically suffer from poor bead-to-bead bonding and relatively high void content, limiting their mechanical properties.

This thesis explores the effect of compaction pressure and temperature on improving the mechanical properties of 3D printed composites. Engineering moduli in the printing and transverse to printing direction, as well as ultimate strength were measured using the tensile testing with Digital Image Correlation (DIC). Tensile testing is performed on the samples that are compacted at different temperatures with pressure. In addition, microscopic studies were carried out to evaluate the void content for different compaction pressures and temperatures. Fiber orientation state was measured for different sets of samples. Differential scanning calorimetry (DSC) was carried out to calculate the degree of crystallinity and possible changes in crystalline morphology as a result of annealing temperature profile.

The results indicate that by selecting appropriate heat treatment profiles both strength and modulus of 3D printed composites can be significantly improved. Strength was improved by over 50% and 100% in printing and transverse directions respectively, and twofold increase of the modulus in printing direction was found. In this respect, the observed mechanical behavior will be

explained in terms of various parameters such as degree of compaction, crystalline structure, orientation state and void content.

ACKNOWLEDGEMENTS

My sincere thanks to Dr. Kravchenko for giving me an opportunity to work with him and guiding me with his knowledge and feedback. I would not have been able to complete this research without Dr. Kravchenko and without funding assistance provided by the ODU Mechanical and Aerospace Department. A special thanks to my friends in the composite research lab who have supported me in learning about the usage of DIC and tensile testing and giving their feedback on my work. I thank all my family members, my teachers, my friends for their constant support and trust. Lastly, I would like to thank my Mom and Dad, who have been an inspiration and supported me in every stage.

TERMINOLOGY

PA 6: Polyamide 6/Nylon

PS: Pristine

AN: Annealing

AC: Annealing with compaction

00: Samples with 0-degree print orientation

90: Samples with 90-degree print orientation

DIC: Digital Image Correlation

DSC: Differential Scanning Calorimetry

Contents

LIST OF TABLES

LIST OF FIGURES

CHAPTER 1

INTRODUCTION

Traditional fabrication processes for composite materials, such as autoclave molding prepreg laminates have geometrical restrictions and are very labor intensive [1]. Injection and compression molded composites allow geometrical complexity but do not have as desirable material properties as prepreg laminates due to poor control of fiber orientation [2]. With these disadvantages of conventional manufacturing processes, there is a need for a fabrication process that can create complex geometries yet still retain the control of fiber orientation to achieve the desired material properties.

Fused deposition modeling (FDM) 3D printing is an additive manufacturing (AM) process in which a filament is extruded through a heated nozzle to build an object layer by layer. This process has recently gained interest due to its versatility, ability for rapid prototyping of geometrically complex parts and the ability to create parts which were not previously possible. Generally, the filament used is a thermoplastic, however, composite filaments also exist. Discontinuous-fiber reinforced composites can now be 3D printed by first creating a filament which contains discontinuous-fibers [3]. Continuous fiber composites can also be 3D printed. Two common methods for printing continuous fiber composites are dual extrusion, in which the fiber and matrix are extruded separately, and nozzle impregnation [4].

The mechanical properties of 3D printed polymer parts have been studied by many authors. Parameters such as printing direction, layer thickness, infill degree and feed rate have a considerable effect on the quality and performance of 3D printed polymer parts [5],[6],[7].

Thermoplastics are used in a wide range of applications because of their high strength, lightweight and relatively low processing costs and PA 6 is one of them. Additionally, nylon-glass fiber composites exhibit excellent strength and good dimensional stability compared with unmodified grades of nylon [8]. Nylon-glass fiber is a high-quality filament with short fiber reinforcement, which is odorless during the extrusion process [9]. Glass fiber filament is ideal for engineering prototypes that require structural mechanical properties and heat resistance [10].

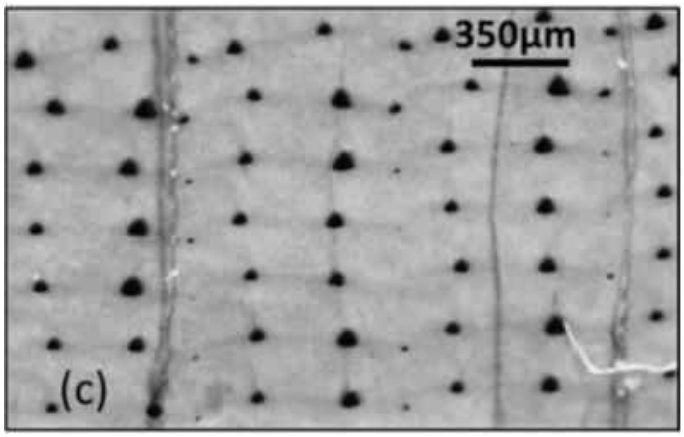

Figure 1:Micrograph depicting the layer arrangement and interlayer voids. [12]

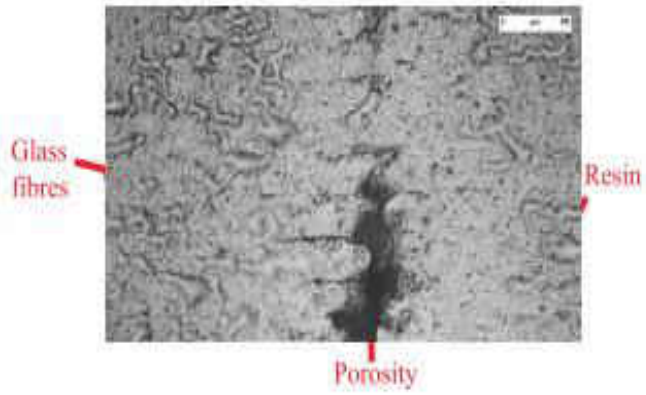

Figure 2: Micrograph of a laminate made of glass fiber/nylon composite [13]

With the recent advancement of 3D printing, polymer composites can be fabricated rapidly for structural and prototyping purposes. However, the mechanical properties of 3D printed polymer composites are typically lower than in composites manufactured using injection molding process. One of the reasons is due to poor degree of bonding between the individual deposited beads (Fig 1) [11],[12]. When the material is printed layer by layer by extruding the filament, the final parts of the material are very porous (Fig 2) [13]. Also, the 3D printed nylon-glass fiber composites inherently exhibit anisotropic properties due to the 3D printing. The short glass fibers are aligned significantly along the printing direction [14]. Therefore, it is necessary to study the effect of post treatment, such as annealing and compaction, on the mechanical properties of nylon-glass fiber composite [15] both in-printing and transverse direction. The heat treatment of the 3D printed composites is followed by heating the sample up to the specified temperature below its melting point and held at that constant temperature for a period of time and then cooled to the ambient temperature [16]. A change in the crystalline structure of the polymer can be observed [17]. This treatment is well suited for the 3D printed parts which results in the release of residual stresses induced during additive manufacturing. Annealing the polymer above the glass transition temperature helps to recover the reduction of interlaminar tensile strength from the additive manufacturing [17]. The focus of this research is to understand how these composites can be strengthened by annealing and compaction. The strength of these composites was determined using tensile testing. Tensile testing is one of the conventional methods used to find the mechanical properties of the material. It provides information on the tensile strength and modulus of the specimens. The fractured surfaces of these tensile tested samples were used to study the volume fraction of the voids, as well as fiber orientation.

CHAPTER 2

METHODOLOGY

The main aim of this thesis is to observe the change in strength of the glass fiber reinforced PA6 composites. Samples treated at different temperatures and pressures are compared with the pristine ones. Samples with 0^0 and 90^0 fiber orientation are considered for experiment. The setup will be discussed, followed by the manufacturing and testing of materials.

A 3Dimensional object is processed from a computer file which consists of G code using Prusa MK3 i3 3D printer (Fig 3), where the part is built by the deposition of material layer by layer which is why it is also called additive manufacturing. The 3D CAD model with the necessary dimensions is converted into a G Code file using Slicer and/or Ultimaker Cura software. The parameters such as print speed, temperature of the extruder and the bed, flow rate, infill direction, layer thickness is set using this software. In case of presence of excess material, it can be removed by using water jet cutting which uses water of high pressure along with abrasive materials. This kind of material removal is called subtractive manufacturing. ProtoMAX software is used to control and guide the water jet cutting machine.

Figure 3. 3D printer used for additive manufacturing

3D printed specimens were grouped into sets and each set of specimens is annealed and annealed with compaction at different temperatures. Annealing was carried out in an oven. Annealing with compaction was carried out using two different methods. The first method used compression molding press to provide uniform heat distribution with controlled temperature and pressure. Another method uses a pressure vessel called autoclave, which is the most common method for curing composites. In the autoclave process, high pressure and heat are applied to the part through the autoclave atmosphere. A specific compaction cycle can be programmed. A vacuum bag was used to apply additional pressure and aid in composite consolidation and reducing the void content.

All the specimens including the pristine, annealed, annealed with compaction, are tested using MTS. Here, the dog bone specimens are placed vertically using fixtures which are attached to the top and bottom head of the MTS machine. When the tensile load is applied continuously, the top head of the fixture moves gradually and stops when the material fails. Data such as force applied, percentage of strain is recorded, stress vs strain curves are generated. Later, the modulus value for each set of samples is calculated.

Digital Image Correlation (DIC) is an optical method which is used to measure the deformation on an object's surface. The movement of applied surface patterns is tracked during the tensile testing using MTS. A series of images is obtained from the beginning till the end of the experiment. It gives the strain values across the entire surface. The strength obtained from the MTS and the strain from the DIC are plotted to get the modulus. This modulus from the DIC is compared with the modulus obtained from the MTS.

All the data from the tensile testing was recorded through Testworks4 software which controls the moving head of the tensile testing machine and is imported into MS-Excel. The stress vs strain curves are plotted which gives the modulus. The stress, strain and modulus are compared using a bar chart.

The fractured surfaces of the samples obtained from the tensile testing machine are studied for the volume fraction of voids and fiber orientation. The samples were cut using a water jet cutter up to 0.5" each including the fractured surface. The samples were polished to allow for microstructural analysis. These polished samples were observed under an optical microscope and the micrographs were analyzed using ImageJ software. ImageJ is an image processing software where these 2-dimensional microscopic images can be studied by adjusting the threshold and by finding the area of fibers, matrix and voids.

Differential scanning Calorimetry (DSC) is carried out on the 3D printed samples to study the temperature profile. DSC is used for a various application including the determination of heat of fusion, crystallization, glass transition temperature T_g, oxidation and other chemical reactions. A heat flow versus temperature curve is obtained from the DSC analysis. The degree of crystallinity for the nylon can be calculated by using the net enthalpy values from the endothermic and exothermic peaks obtained from the DSC curves.

2.2. Experiment Setup

2.2.1. Sample Manufacturing

The material used is XSTRAND GF30-PA6 with a filament diameter of 1.75mm and melting temperature of 206C. This material comes in large rolls, in the form of filaments (Fig 4). The filament is made up of Polyamide6/nylon matrix reinforced with 30% of glass fibers. The filament is dried for up to 4hr in the oven at 80°C before using for better printing results. The filaments were fed into the 3D printer where it is melted and is extruded in the form of layers [18]. The printing is carried out at a printing temperature of 250°C and at a speed of 30mm/s with a printing bed at 90°C.

Figure 4. Filament used for 3D printing [19]

The nylon glass fiber composites that are used for testing are manufactured in the form of dog bones. The 3D model of each dog-bone specimen is designed using Autodesk Inventor and is sliced using Ultimaker Cura. The sliced model is fed into the 3D printer in the form of g code. Each dog bone model is manufactured using an additive manufacturing process in which it is 3D printed layer by layer with a gage dimension of 60x10x3.2mm (Fig 6) with each layer thickness being 0.2mm. The structure dimension of the specimen is followed by the ISO 527-2 which provides similar results to the ASTM D638.

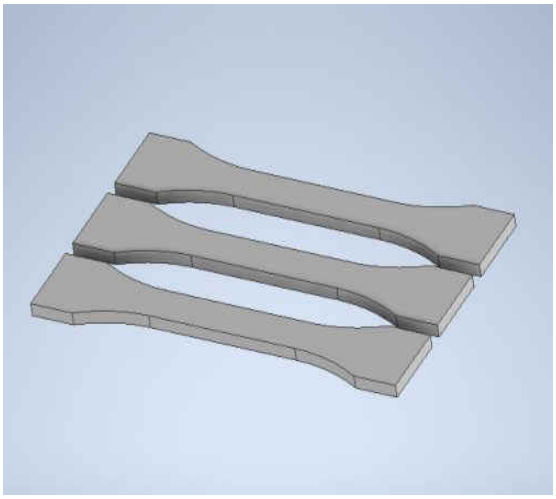

a.

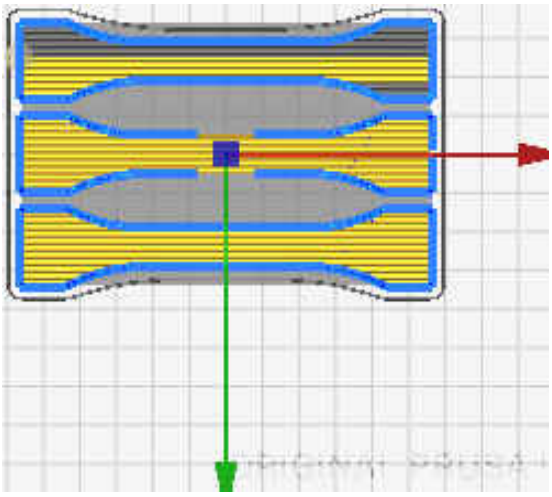

b.

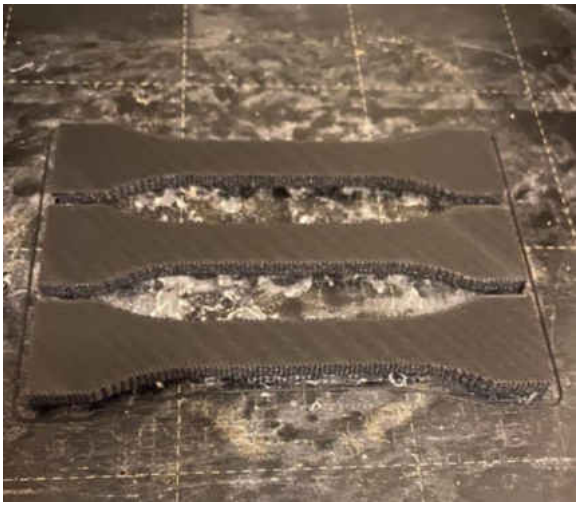

c.

d.

Figure 5. a. Dimensional model designed using Autodesk Inventor; b. Preview of the sample from the Ultimaker Cura; c. 3D printed sample; d. Painted samples before tensile test

Figure 6:3D printed dog bone sample.

2.2.2 Heat Treatment

3D printed dog-bone samples are categorized into groups for the annealing process with/without compaction as mentioned in the Table 1.

Annealing is one of the several heat treatment processes used in polymer manufacturing to increase the strength of the materials. The annealing process has shown a great advantage when applied to polymer composites, wherein the composite material becomes stronger after annealing. This process will lead to increase in the properties of 3D printed samples by distributing the stress more evenly thus decreasing its chances of quick fracture by increasing the tensile strength [20].

Annealing of the 3D printed samples was carried out in a closed oven. The oven is pre heated up to 100C to 150C and then the samples were covered with a release film to prevent the sample from adhering to the inner panel of the oven. Annealing the samples along with a pressure of 80psi was carried out in a closed vessel called the autoclave. Annealing with compaction for some of the samples was carried out using hot press (Fig 7). The heat press contains two heated

platens. The vacuum bagging setup is placed between the heated platens as shown (Fig 8). The pressure is applied in terms of tons of force by taking the surface area of the sample into consideration. (1psi= 4.464E-4 ton-force/square inch). After the heat treatment, the heat supply for the heated platens and the pressure are turned off. The samples are taken out only after they are cooled down to a room temperature to avoid warping.

Figure 7: Heat press used for heat treatment.

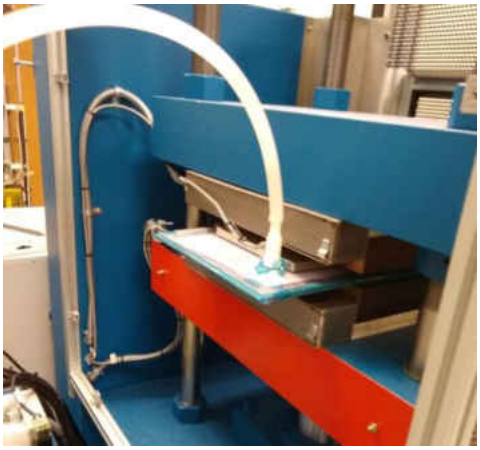

Figure 8:Vacuum bagging setup with heated platens.

Table 1: Number of specimens tested per group treated at different temperature and pressure

Print orientation	**Pristine**	**Annealed without compaction**			**Annealed with Compaction (80 psi)**		
		150° C	**170° C**	**200° C**	**150° C**	**170° C**	**200° C**
0 degree	3	3	3	3	6	3	5
90 degree	3	3	3	3	6	3	5

2.2.3 Vacuum Bagging

Vacuum bagging is one of the most ancient and easiest methods to consolidate fiber reinforced polymers. The 3D printed samples were placed on a base plate(aluminum) with a release film on top and bottom in such a way that the sample, when heated at high temperature does not stick to the base plate. The whole setup (Fig 9) is covered using a vacuum bag in which a breather is used in between the sample covered with release film and the top vacuum bag layer. This

breather enables the whole vacuum bag to path through the vacuum source. Volatile gases and air can easily escape through this breather and the pressure applied can be distributed evenly throughout the vacuum bag.

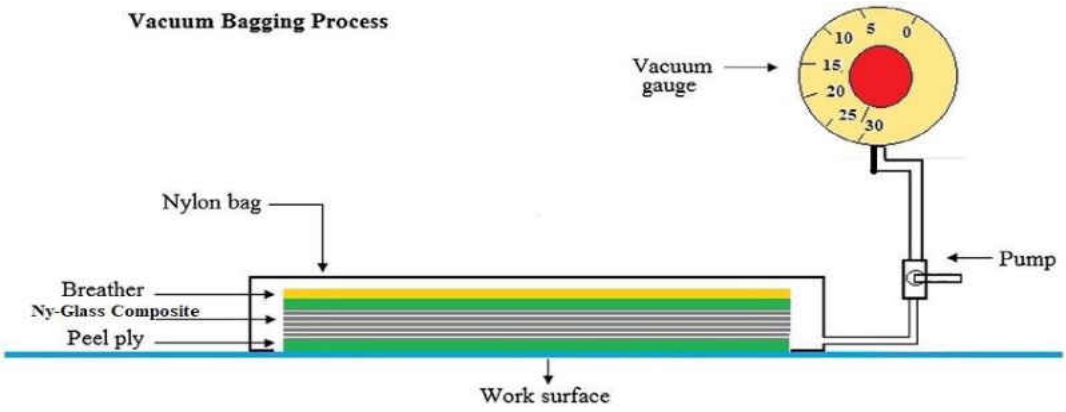

Figure 9: Vacuum bagging set up

Figure 10:Vacuum bagging setup-before and after heat treatment

2.3 Tensile Testing

The tensile testing of the specimens was conducted using MTS with a load cell of 300kN (Fig 11). The samples were designed in the form of dog bones and the tabs of the dog bones were designed for easy gripping [21]. During tension, one of the tabs were attached to a fixed position and the other attached to a crosshead moving at 0.2mm/min until the fracture of the sample (Fig 12). Each of these samples were clamped in fixtures that are designed for even load distribution along the cross section of the specimen. The MTS machine used for tensile testing is equipped with TestWorks4 software to achieve constant speed in tension.

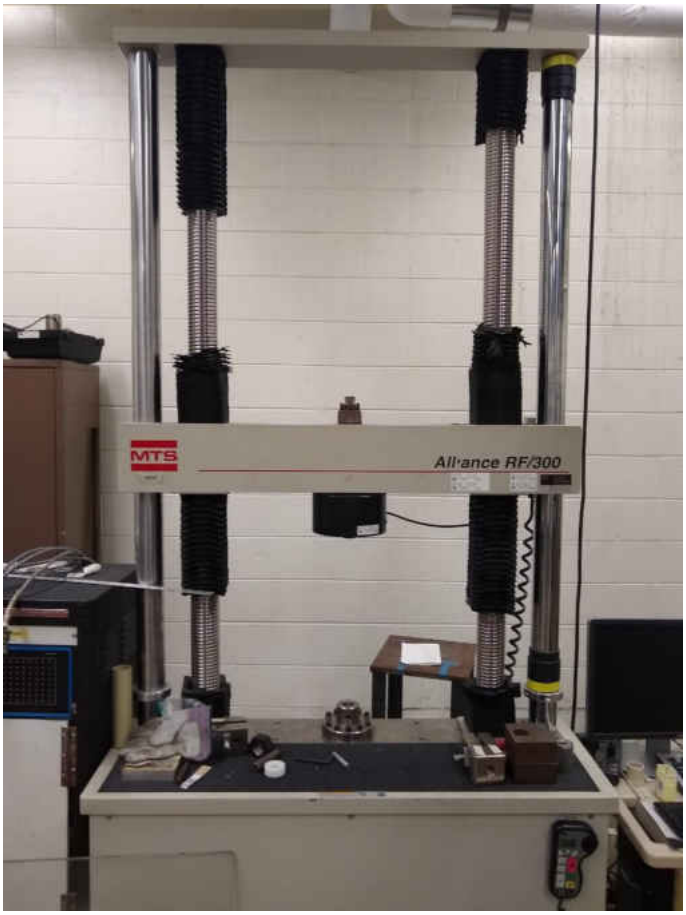

Figure 11: MTS machine used for tensile testing

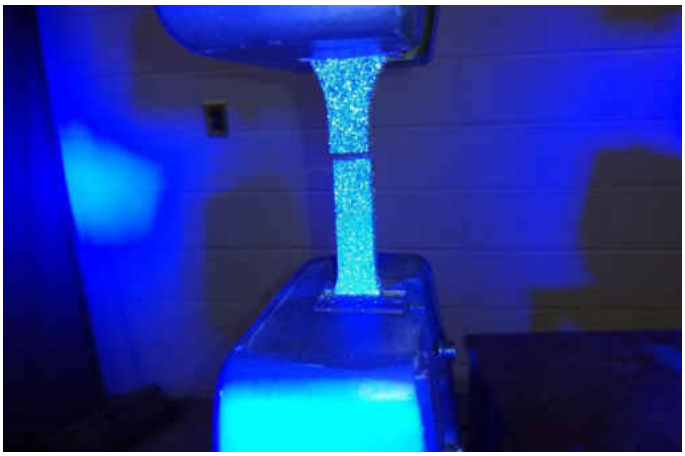

Figure 12: Tensile testing setup with DIC

2.4 Digital Image Correlation

Digital Image Correlation is a software used for optical tracking of the deformation of the sample during tensile testing. The setup consists of an acquisition DIC software-GOM correlate, a high-quality camera which is focused on the specimen (Fig 13). The area/region on the specimen which is subjected to tensile load is selected (Fig 14), and then the whole cycle is recorded using the software. The percentage strain along the length of the specimen is thus recorded from the software at intervals of 10 seconds. The strain values from this are used to plot the stress vs strain curves and to calculate the tensile modulus of each sample.

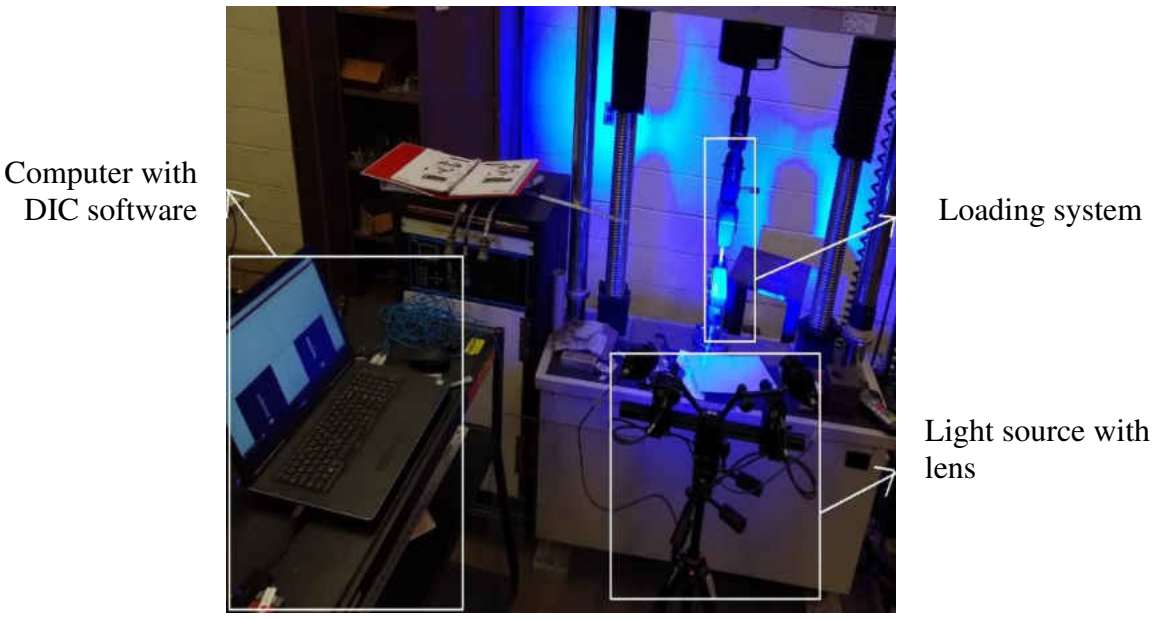

Figure 13: DIC set up

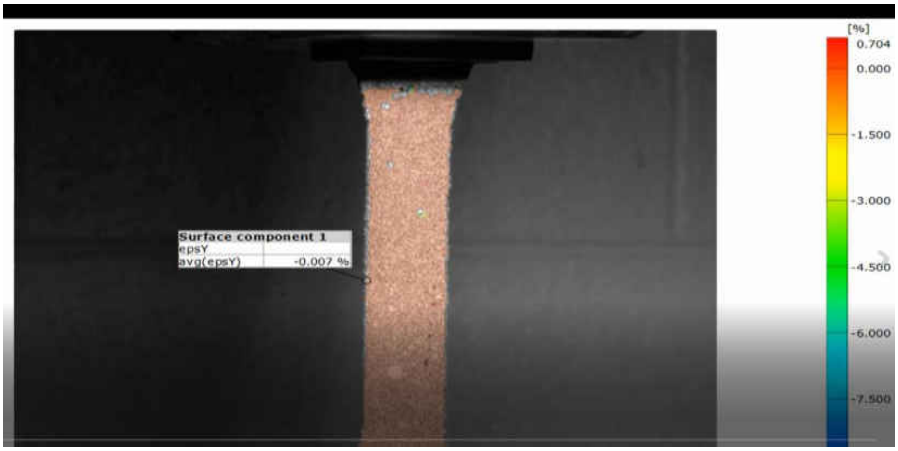

Figure 14:Image showing the strain rate recorded from the GOM software during tensile testing.

2.5 Microscopic Studies on Cross Section

The microscopic studies were carried out on the polished cross section of the Ny-glass composite specimens using an optical microscope [22]. A small portion of the sample, approximately 0.5" including the fractured end were cut using a water jet cutter and mounted in resin for grinding and polishing. These polished samples are dried to obtain a clearer cross-sectional image of the fractured surface (Fig 15). High quality images obtained from the microscope are analyzed using ImageJ software.

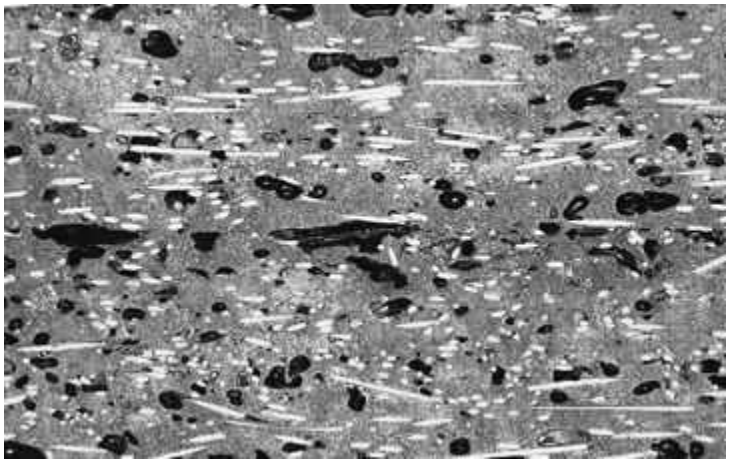

Figure 15:Polished cross section micrograph captured from optical microscope

2.5.1 Evaluation of Fiber Distribution

The images captured from the optical microscope were saved in a jpeg format and imported into the ImageJ software. These images were converted into grayscale (Fig 16) and the area of fibers, matrix and the voids can be found by selecting the particles. In the (Fig 16), all the fibers were shown in white and the rest of the black region consists of voids and the resin. The area of the white region and the black region is calculated using ImageJ software which refers to the area of the fibers and the matrix including voids respectively.

The image (Fig 15) is adjusted in such a way that the voids are represented in white and the rest of the black region consists of fiber and matrix.

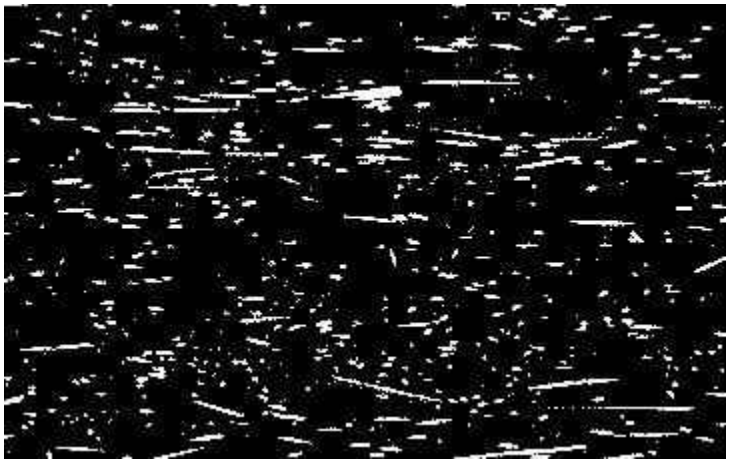

Figure 16:Microscopic image showing the fibers in white.

Figure 17:Microscopic image showing the voids in white

2.5.2 Evaluation of Fiber Orientation

The fiber orientation is found using the same ImageJ software that was used to calculate the volume fraction of voids. The image with higher magnification is used for analyzing the orientation of fibers. The threshold of the micrograph is adjusted by following the same procedure that was followed to find the volume fraction of voids as shown in figure (Fig 17). Each fiber and/or void is selected, and the ellipses were fitted into the ellipses. The parameters such as area,

length and width of the ellipse were recorded from the software *Analyze>Analyze Particles>Ellipses (Exclude on edges, Display Results)*. These parameters were used to calculate the fiber orientation in each micrograph.

To find the fiber orientation in a composite.

The Formulae that are used are as follows:

$$\boldsymbol{A_{ij}} = \begin{bmatrix} \boldsymbol{a_{11}} & \boldsymbol{a_{12}} \\ \boldsymbol{a_{21}} & \boldsymbol{a_{22}} \end{bmatrix}$$

$$\boldsymbol{a_{ij} = p_i p_j}$$

$$\boldsymbol{p_i} = \begin{bmatrix} \boldsymbol{cos\psi_i} \\ \boldsymbol{sin\psi_i} \end{bmatrix}$$

$$\boldsymbol{\psi_i = \mathbf{acos}\left(\frac{h_i}{l_i}\right)}$$

$$\boldsymbol{\psi_i = \mathbf{acos}\,(h_i/l_i}$$

where h_i and l_i are the minor and major axes, respectively. A_{ij} matrix represents the fiber orientation.

2.6 Differential Scanning Calorimetry

Differential Scanning Calorimeter is used to measure the amount of heat required to raise the temperature of the sample. This technique was carried out by considering the heat flow in the sample and a reference pan. The sample that was considered here was nylon-glass fiber composite. The difference in the amount of heat absorbed or released between the sample and the reference is directly measured as a function of temperature during phase transitions. Power Differential DSC and Heat flux DSC are the two types of Differential Scanning Calorimetry. Power Differential DSC is carried out by maintaining the same temperature on both the sample and the reference and

the power required to obtain and maintain the temperature is recorded. Whereas in Heat Flux DSC, the same temperature is maintained for both sample and the reference and the difference between the heat supplied to maintain that temperature is recorded. Heat Flow versus Temperature curve is obtained from DSC. This change in heat flow can be calculated by integrating the ΔT_{ref} curve (Fig 18). The DSC profile shown in the curves (Fig18), is heating-cooling-heating-cooling. A heating rate of 10^{o}C/min was used with nitrogen atmosphere around the sample with a flow rate of 50mL/min.

Crystallinity refers to the degree of structural order in a material and strongly affects its properties such as strength, density, and Young's modulus. Higher value of degree of crystallinity refers to the regularity of chains oriented in the sample. Additionally, higher degree of crystallinity reduces the amorphous phase and typically leads to higher mechanical properties. The enthalpy of 100% crystalline PA6 depends on the polymerization process of the PA6 is 135 J/g for anionic ring opening polymerization, which is the most common for PA6 [23]. Therefore, the degree of crystallinity can be found by considering the area under the heat flow curve during the first melting DSC cycle and normalizing it with the adjusted enthalpy value for 100% crystallinity. Based on the glass fiber weight fraction of 30% in 3D printed composite the adjusted enthalpy is 94.5 J/g.

Upon this calculation the following degrees of crystallinity were found:

- As printed: 32.05/94.5 = 0.34 = 34%
- Annealed at 170^{0} C: 38.10/94.5 = 0.403 = 40.3%
- Annealed and compacted at 200^{0} C: (30.69 + 12.69)/94.5 = 0.46 = 46%

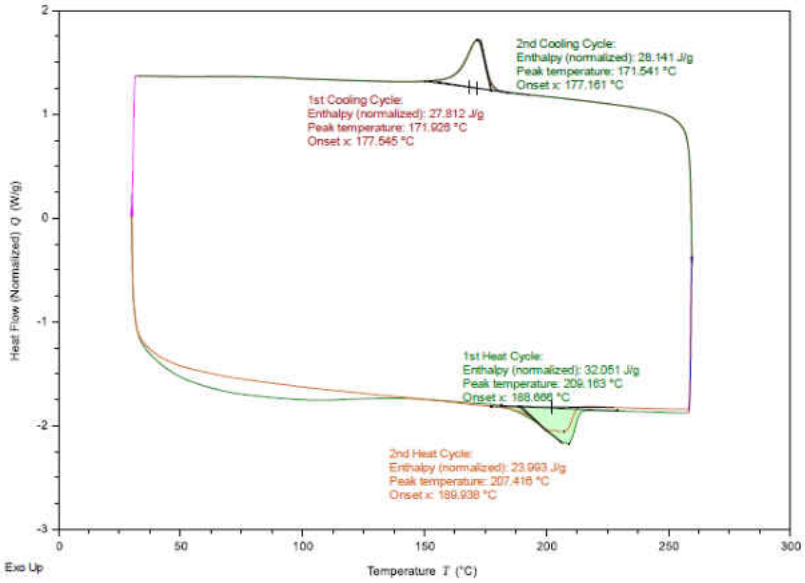
2nd Cooling Cycle:
Enthalpy (normalized): 28.141 J/g
Peak temperature: 171.541 °C
Onset x: 177.161 °C
1st Cooling Cycle:
Enthalpy (normalized): 27.812 J/g
Peak temperature: 171.926 °C
Onset x: 177.545 °C
1st Heat Cycle:
Enthalpy (normalized): 32.051 J/g
Peak temperature: 209.163 °C
Onset x: 188.666 °C
2nd Heat Cycle:
Enthalpy (normalized): 23.993 J/g
Peak temperature: 207.416 °C
Onset x: 189.938 °C
Heat Flow (Normalized) Q (W/g)
Exo Up
Temperature T (°C)

a.

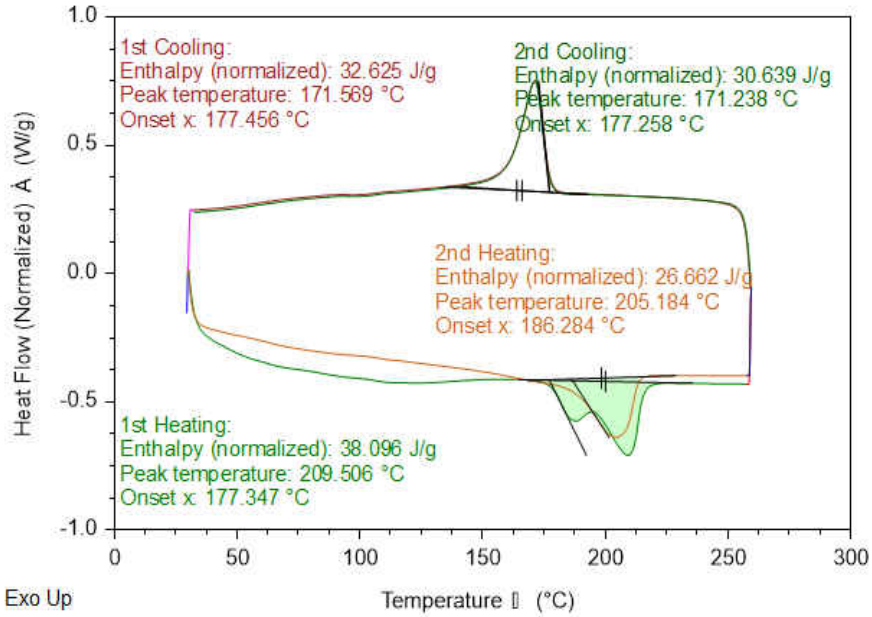
1st Cooling:
Enthalpy (normalized): 32.625 J/g
Peak temperature: 171.569 °C
Onset x: 177.456 °C
2nd Cooling:
Enthalpy (normalized): 30.639 J/g
Peak temperature: 171.238 °C
Onset x: 177.258 °C
2nd Heating:
Enthalpy (normalized): 26.662 J/g
Peak temperature: 205.184 °C
Onset x: 186.284 °C
1st Heating:
Enthalpy (normalized): 38.096 J/g
Peak temperature: 209.506 °C
Onset x: 177.347 °C
Heat Flow (Normalized) Â (W/g)
Exo Up
Temperature Ï (°C)

b.

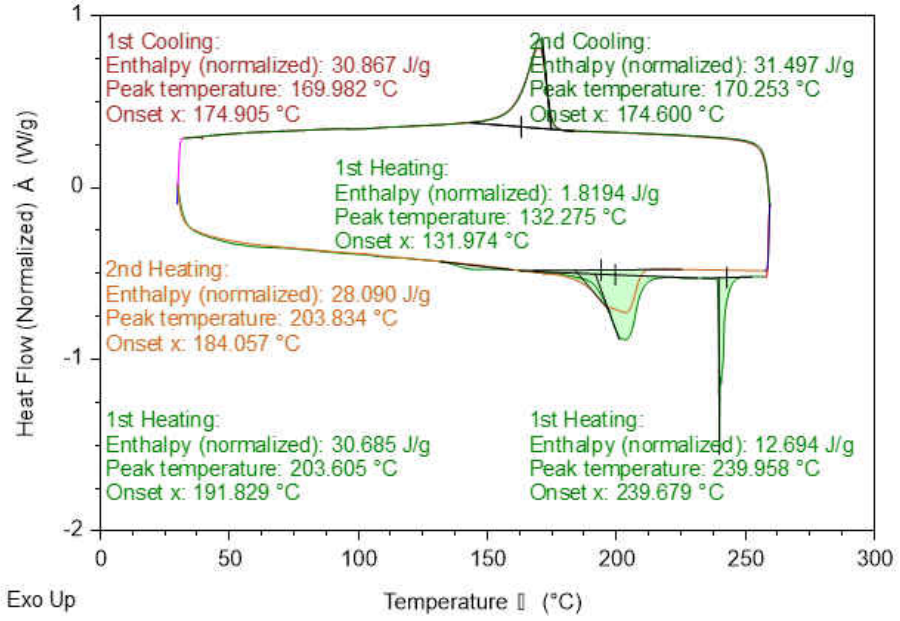

c.

Figure 18:DSC Curves for pristine (a), annealed at 170^0 C (b) and annealed with compaction at 200C (c)

The significant increase of degree of crystallinity was observed with increased annealing temperature from 34% for pristine to 46% for annealed at 200 C.

Another noticeable difference was observed in the shape and temperature of the melting peaks, corresponding to phase transition enabled by thermal treatment [24]. This phase transition, especially in sub-Tm region has been shown to correspond to the improved mechanical properties of nylon 6 [25].

CHAPTER 3

RESULTS AND DISCUSSION

Load vs elongation data was obtained using TestWorks 4 software and then exported to a spreadsheet for post processing. This data is used along with the original dimensions of the specimen to construct a stress strain diagram. The mechanical properties such as modulus, ultimate tensile stress was determined for each set of specimens. The results for each set of samples were compared using tabulated means. On the other hand, the strain data obtained from the DIC plotted vs the stress obtained from the TestWorks 4 which will generate the modulus. The modulus values obtained from both the methods are compared.

3.1 Effect of Temperature and Pressure

The samples showed a change in their dimension when heat treated and there was a major reduction in the thickness when the pressure was applied. Temperature has played a major effect in increasing the tensile strength of the samples.

3.2 Evaluation of Degree of Compaction

Degree of compaction of the samples tended to decrease when annealed and furthermore a decrease in thickness was observed when they were compacted at a higher temperature of 200° C. The average thickness of the printed samples was found to be approximately 3.2mm and there was a decrease in thickness ranging from 0.04mm to 0.74mm for 0 degree samples (Fig 19) and 0.13mm to 0.60mm for 90 degree samples (Fig 20). Among all the samples with 0-degree print orientation, the samples annealed at 200C with compaction exhibit an increase in degree of

compaction. It can be concluded that as the temperature is raised near to the melting point of the composite along with pressure, the thickness of the composite material decreases. This is because the annealing process along with compaction will result in the distribution of heat evenly throughout the composite and the release of residual stresses introduced during 3D printing.

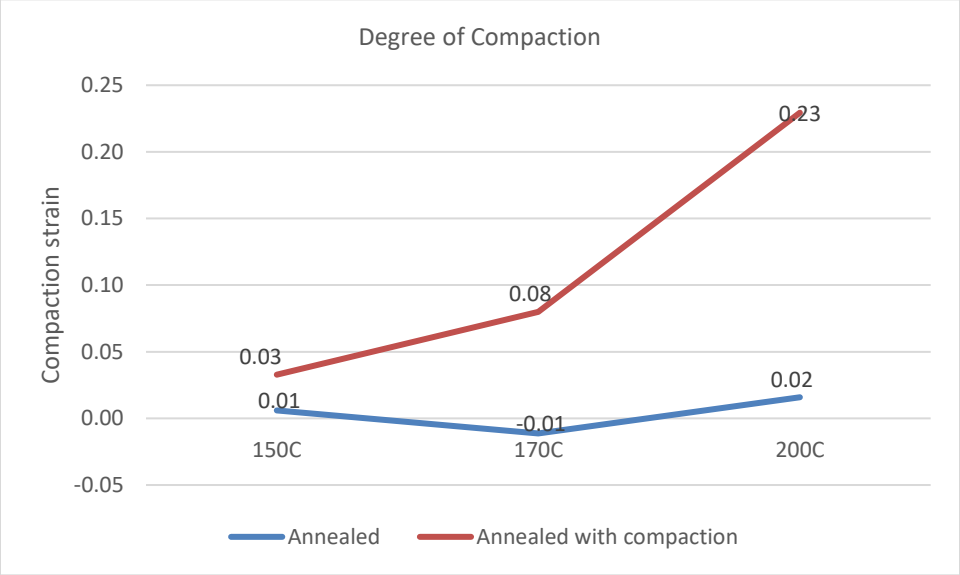

Figure 19:Degree of compaction for samples with 0-degree print orientation.

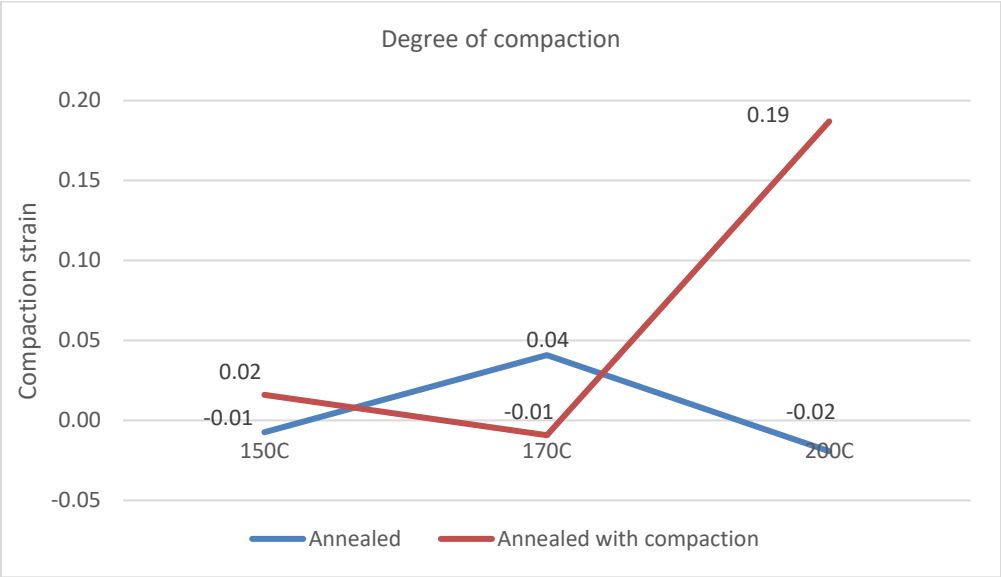

Figure 20::Degree of compaction for samples with 90-degree print orientation.

3.3 Stress Strain Curves

The (Fig 21) shows the stress strain curve obtained from the tensile test on PA6 specimens. The curve shows that the tensile strength increases with increase in strain and shows brittle fracture as shown in (Fig 21). The tensile modulus is obtained by calculating the slope of the linear region of the curve as represented in the figure. Similarly, Young's Modulus for each sample is calculated and their averages are compared.

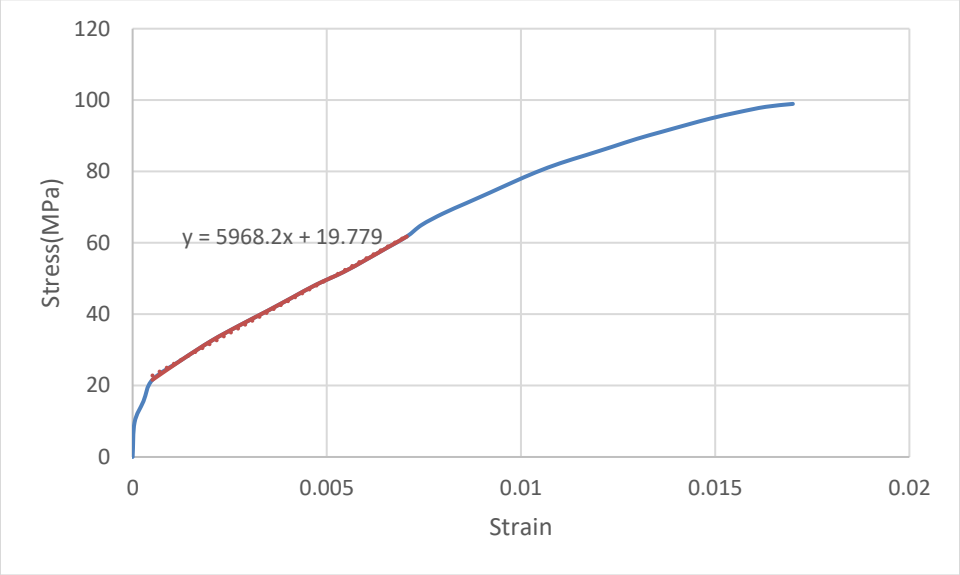

Figure 21:Stress strain curve for one of the annealed samples

3.4 Stress Strain Curves for Material Compacted and Annealed at Different Temperatures

Samples compacted with 80psi tend to have higher strength of approximately 100MPa for 0 degree and 60MPa for 90 degree print orientation when annealed at 200°C than those annealed at 150°C and 170°C for both 0 degree and 90 degree print orientation (Fig22) along with higher value of strain.

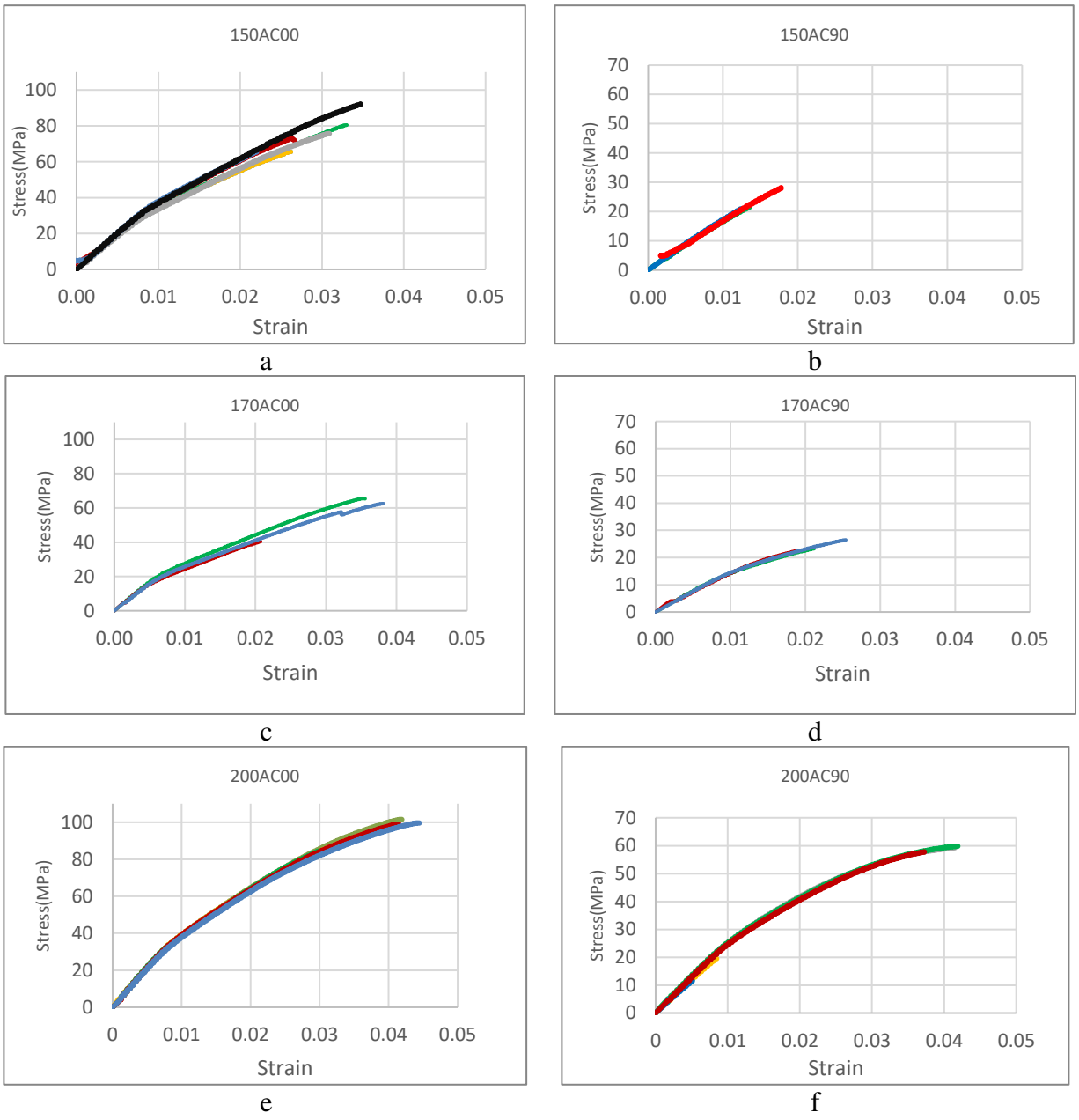

Figure 22:Stress Strain curves of 0-degree (Left) and 90-degree (Right) samples annealed at temperatures 150°C: a) and d),170° C: b) and e) and 200° C: c) and f) with pressure of 80psi.

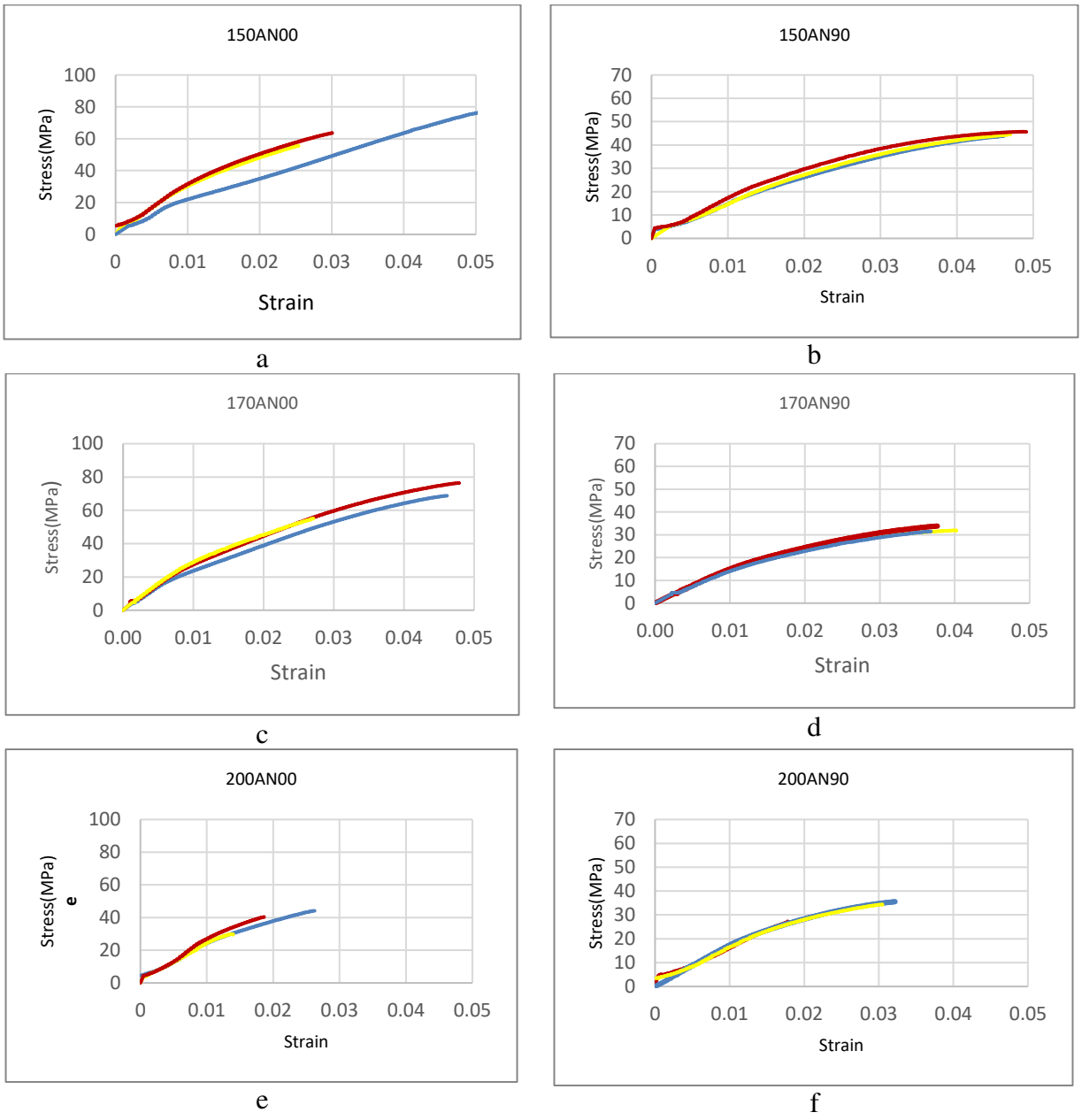

Figure 23:Stress Strain curves of 0-degree (Left) and 90-degree (Right) samples annealed at temperatures 150°C: a) and d),170° C: b) and e) and 200° C: c) and f) without pressure.

It is noticeable (Fig 23) that these 3D printed samples exhibit anisotropic behavior. The samples exhibit higher strength and modulus in the printing direction/0-degree when compared to the transverse direction/90-degree.

3.5 Ultimate Tensile Strength and Engineering Moduli

Load and extension values with respect to time are obtained from the TestWorks 4 Software. The stress was calculated using load values and the horizontal cross-sectional gage area of the specimen. Strain was calculated from the displacement of the crosshead and the gauge length of the specimen. Using the stress vs strain curves, the modulus was obtained for each sample. Also, strain is calculated using the percentage of elongation along the direction of the tensile load recorded from the DIC and the original gauge length of the specimen. These strain values were plotted against the stress values calculated from the TestWorks Software which gives the modulus. A correction factor is calculated by taking the data from DIC and MTS and is applied to the results obtained from the TestWorks. Thus, the tensile modulus for each set of samples are represented using a bar chart as shown in (Fig 24) and Fig (25) with the error bars indicating the single standard deviation for each set of samlples.

The samples follow a trend where there is increase in strength and modulus value as the samples are annealed at 170C-150C and 200C with compaction. It can be observed that there is no such effect on the strength of the samples when they are annealed at 150C with compaction. The change starts at 170C and gives us a better strength and modulus at 200C.

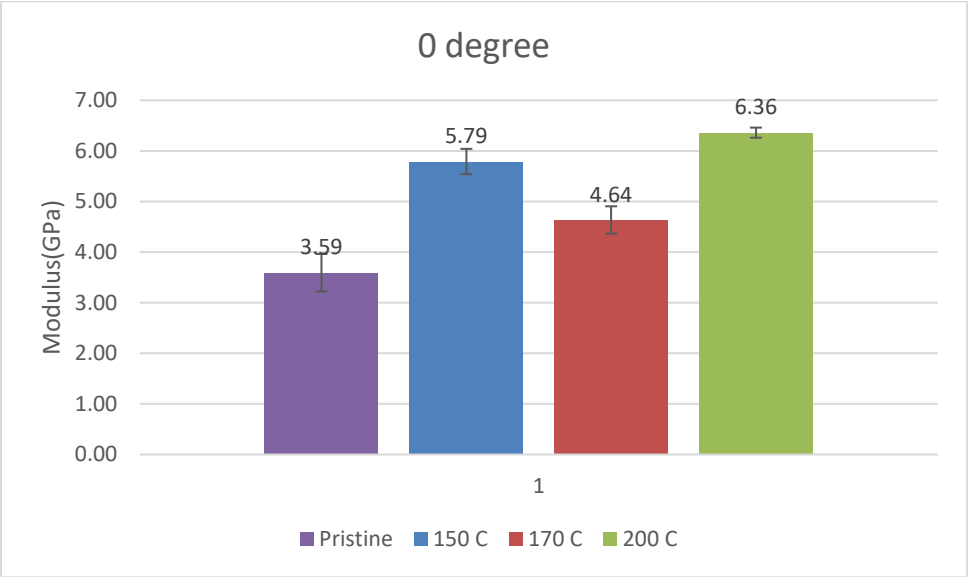

Figure 24: Elastic modulus of 0-degree samples compacted at 80psi and annealed at different temperatures

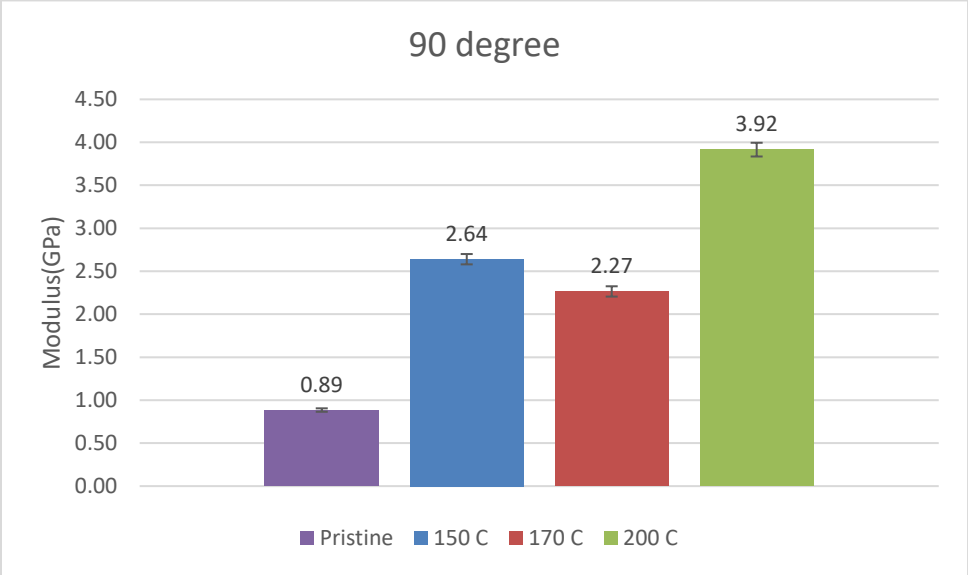

Figure 25:Elastic modulus of 90-degree samples that are compacted at 80psi and annealed at different temperatures.

Fig 24 shows the 0 degree samples that are annealed at 150°C shows a higher modulus of 3.59GPa compared to the 200°C with modulus 6.36GPa and the 170°C being the least of about

4.64GPa, also, Fig 25 shows that the 90degree samples that are annealed at 200°C has a modulus of 3.92GPa which is greater 150°C with modulus 2.64GPa which is also comparatively greater than the ones annealed at 170°C with modulus 2.27GPa. An increase in the modulus is achieved from pristine samples to samples annealed at 200C with compaction. The tensile modulus values for a few samples were discarded because either the DIC strain values were not recorded properly, or the samples were damaged (bent) before testing.

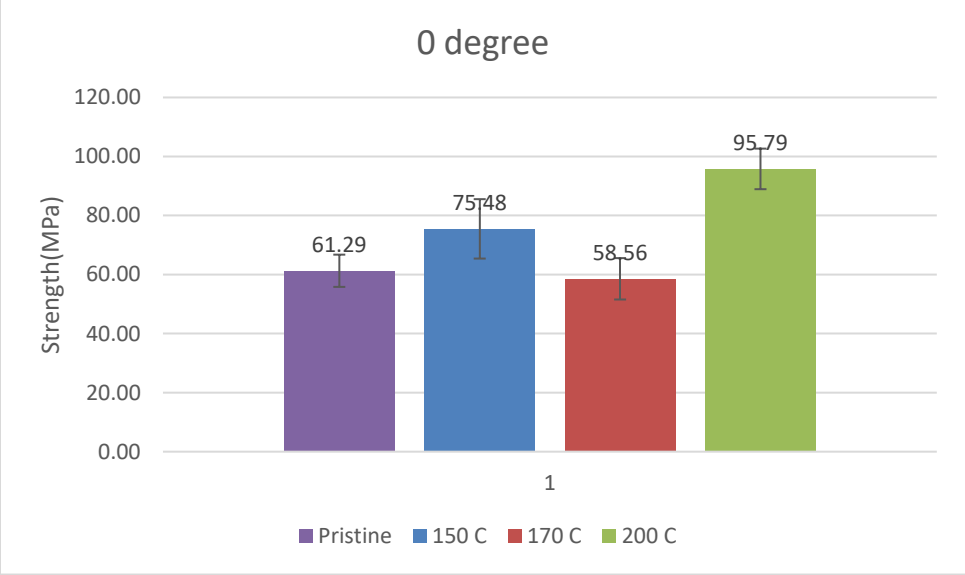

Figure 26:Tensile strength of 0-degree samples that are compacted at 80psi and annealed at different temperatures

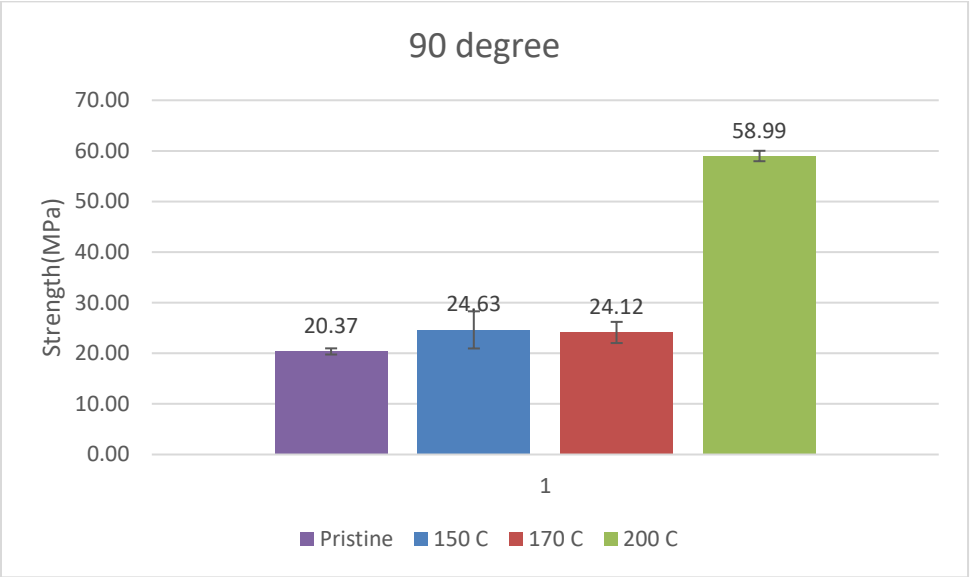

Figure 27:Tensile strength of 90-degree samples that are compacted at 80psi and annealed at different temperatures.

Samples compacted with 80psi at 200°C show extremely high ultimate strength of 95.79MPa (Fig 26) and 58.99Mpa (Fig 27) for both 0-degree and 90-degree print orientation. The samples follow a trend in which the strength of the samples decreases from 75.48MPa to 58.56MPa for 0 degree samples 24.63MPa to 24.12MPa for 90degree samples when the temperature is increased from 150°C to 170°C and then it increases as it reaches the temperature of 200°C which is near to the melting point of the composite, i.e., 206° C. Thus, the strength of the pristine samples- 61.29 MPa for 0degree and 20.37 MPa, increases upon annealing over 170° C. Annealing the samples at 200° C with compaction increases both the strength and modulus of the sample compared to the pristine and samples annealed at 150C with compaction.

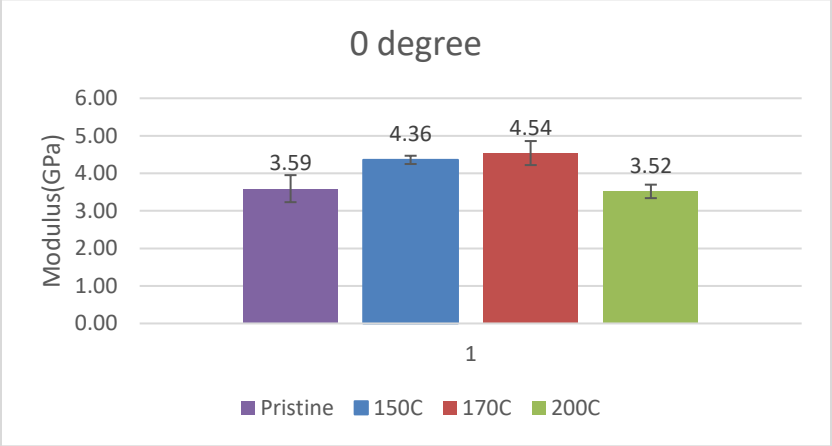

Figure 28:Elastic Modulus of 0-degree samples annealed at different temperature without compaction.

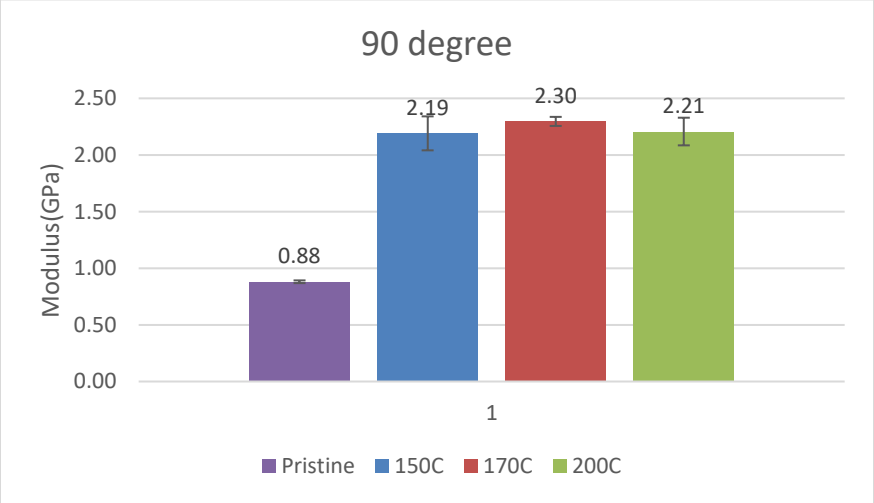

Figure 29:Elastic Modulus of 90-degree samples annealed at different temperature without compaction.

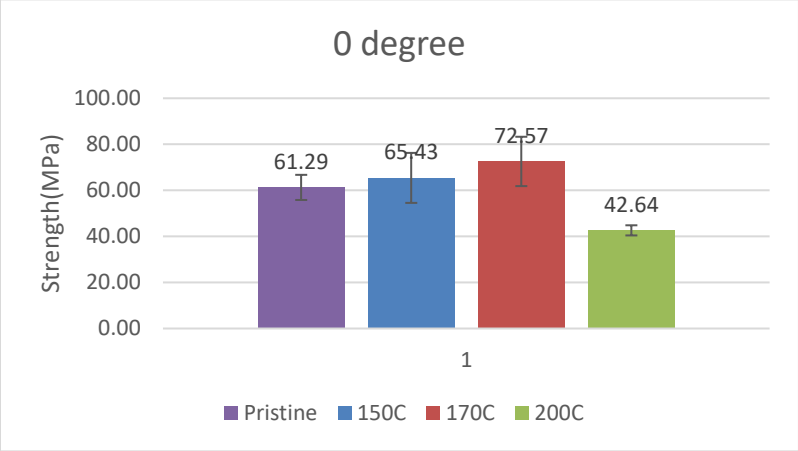

Figure 30:Tensile strength of 0-degree samples annealed at different temperature without compaction.

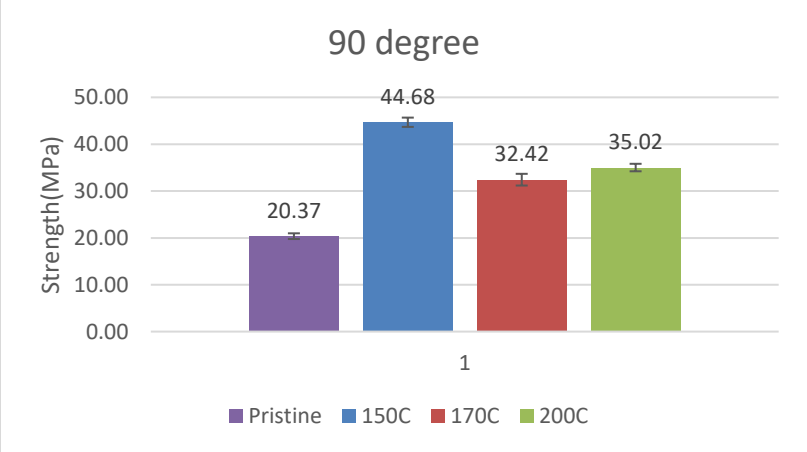

Figure 31:Tensile strength of 90-degree samples annealed at different temperature without compaction.

Annealing of 3D printed samples without compaction does not greatly help in improving the mechanical properties when compared to the ones annealed with compaction. However, an improvement in strength and modulus is observed in samples treated at 150°C and 170°C for both 0- and 90-degree. The reduction in modulus and strength were found for samples annealed at 200°C in both printing and transverse directions. This result is largely due to the following, as sample indicated by DSC the degree of crystallinity has increased significantly, causing

differential re-crystallization shrinkage in the material [26]. This shrinkage results in microscopic cracking of the sample. The evidence of that can be seen for the 170°C annealed sample with and without compaction as well. The micrographs in the following section demonstrate the presence of microscopic voids between the beads. On the other hand, the increase of degree of crystallinity in nylon has been shown to cause more of brittle like behavior [27]. Therefore, both effects can explain why 200°C annealed sample demonstrates reduced properties.

Table 2: Strength and Modulus of samples treated at different temperatures and with/without pressure.

		0 degree				90 degree			
		Strength (MPa)	St.dev (MPa)	Modulus (GPa)	St.dev (GPa)	Strength (MPa)	St. dev (MPa)	Modulus (GPa)	St.dev (MPa)
Pristine		61.29	5.46	3.59	0.37	20.37	0.61	0.88	0.01
Annealed without compaction	150C	65.43	10.86	4.36	0.11	44.68	0.98	2.19	0.10
	170C	72.57	10.72	4.54	0.32	32.42	1.25	2.30	0.04
	200C	42.64	2.20	3.52	0.18	35.02	0.80	2.21	0.22
Annealed with Compaction (80psi)	150 C	75.48	10.06	3.86	0.17	24.63	3.67	2.64	0.06
	170 C	58.56	7.01	4.64	0.26	24.12	2.09	2.27	0.06
	200 C	95.79	6.87	6.36	0.11	58.99	1.03	3.92	0.075

3.5.1 Statistical Significance Test

Table 3: p-values obtained from t-test for comparison of modulus of pristine and samples with other heat treatments.

	Pristine	Annealed			Annealed with compaction			p-value	
		150	170	200	150	170	200		
Modulus 0-degree, GPa	3.59	4.36						0.0129	Significant
			4.54					0.0141	Significant
				3.52				3.7109E-06	Significant
					5.79			0.081	Not Significant
						4.64		0.0079	Significant
							6.36	1.6559E-06	Significant
Modulus 90-degree, GPa	0.88	2.19						1.1396E-05	Significant
			2.30					2.3648E-07	Significant
				2.21				0.0002	Significant
					2.64			1.9815E-10	Significant
						2.27		1.2172E-06	Significant
							3.92	3.5007E-10	Significant

Table 4:: p-values obtained from t-test for comparison of strength of pristine and samples with other heat treatments.

	Pristine	Annealed			Annealed with compaction			p-value	
		150	170	200	150	170	200		
Strength 0-degree, MPa	61.29	65.43						0.2934	Not Significant
			72.57					0.08984	Not Significant
				42.64				0.0026	Significant
					75.48			0.0303	Significant
						58.56		0.31140	Not Significant
							95.79	0.0001	Significant
Strength 90-degree, MPa	20.37	44.68						1.6861E-06	Significant
			32.42					5.7459E-05	Significant
				35.02				7.3356E-06	Significant
					24.63			0.0473	Significant
						24.12		0.0203	Significant
							58.99	8.82344E-10	Significant

A statistical significance t-test was carried out on the strength and modulus of the samples treated at different temperature conditions. A one tailed t-test with two independent means was carried out with 95% confidence level. A significance level, $\alpha=0.05$ was chosen and the p-vales are reported (Table3 and Table 4). The single standard deviation of each set of samples are represented by error bars in each of the bar charts (Fig 25 to Fig 31). This independent samples t-test was conducted to compare the strength and modulus of pristine samples with each of the sample set treated at different temperature and pressure.

The t-test statistic values can be calculated from the following equations:

$$S_p^2 = \frac{(n_1 - 1)S_1^2) \ + \ (n_2 - 1)S_2^2}{n_1 + n_2 - 2}$$

$$t_0 = \frac{\overline{y_1} - \overline{y_2}}{S_p\sqrt{\frac{1}{n_1} + \frac{1}{n_2}}}$$

where,

S_p^2 is the pooled variance assuming equal variances in the samples

y_1 and y_2 are the means of the independent samples

n is the sample size and (n-1) refers to the degrees of freedom.

p-values were calculated in excel by considering a one tail t distribution.

Considering the comparison of modulus of pristine samples with one of the sample set, i.e., the samples annealed at 150C. The following assumptions were considered for this case:

A sample size of n_1=3 and n_2=3 was considered for pristine and annealed at 150C without compaction (Table 1).

By using the above equations, t_0 is found to be 3.455081, t_{ref} = 2.131847, which means that the test is statistically significant with p=0.01296694 where p≤0.05.

The p-values for each sample set were calculated using the same procedure by considering the sample size as mentioned in (Table 1). A significant difference in the values for pristine and heat-treated samples can be observed. These results suggest that whether the conditions of the heat treatment used influences the strength and modulus. p-values≤0.05 indicate that the results are statistically significant, and the heat treatment used influences the tensile strength and modulus of the samples. Some of the p-values obtained are >0.05 indicating that the respective heat-treatment used has no significant effect on strength and modulus with 95% confidence level.

The samples annealed without compaction at 170 has p>0.05 indicating that annealing at 170C has no significant effect on strength and modulus in printing direction. This can be explained by the presence of voids from the microscopic analysis conducted on the polished surfaces of the fractured samples and the brittleness caused by the increase in degree of degree of crystallinity.

3.6 Micrograph Analysis

The micrographs for the 3D printed samples were analyzed using ImageJ software. The images obtained from the microscopy have a length scale of 1mm, 2mm and 500µm with a scale bar marked at the bottom right of the image with small line markings (Fig 32a). In case of the below image, the length scale of the image is 2.00mm and 15.0kV is the voltage used to accelerate the electrons while shooting the sample. Before analyzing, the image should be converted to 8-bit mode, *Image>Type>8-bit*. For these types of images, the pixel value ranges from 0 to 255 in which 0 is taken to be black and 255 is taken to be white. The threshold of each image was manually adjusted such that below the set value lies all the fibers and above which the matrix lies. This was done by selecting B&W (Black and White) where fibers were distinguished from the matrix with a dark background *Image>Adjust>Threshold>B&W>Apply*. The image with the set threshold can be compared with the original image manually to differentiate between the fibers and the matrix. With this threshold, the image is converted to binary such that the black background representing the matrix and the white particles representing the fibers *Process>Binary>Make Binary.* These Binary images were analyzed for the area of the Black region (Matrix) using *Analyze>Analyze particles*. The same micrograph is inverted *Edit>Selection>Make Inverse,* such that the area of fibers can be analyzed by following the same procedure. Similarly, the threshold of the image is adjusted such that both the matrix and the fibers are together represented in black and the voids

are represented in white as shown in figure (Fig 32b). This image can be analyzed to find the area of voids using the scale mentioned at bottom right of the image (Fig 32a). and the remaining area will represent the area of the matrix and fibers. Each of these areas including the area of matrix, fibers and voids were used to find the volume fraction of each constituent Table (Volume fraction of matrix, fibers and voids).

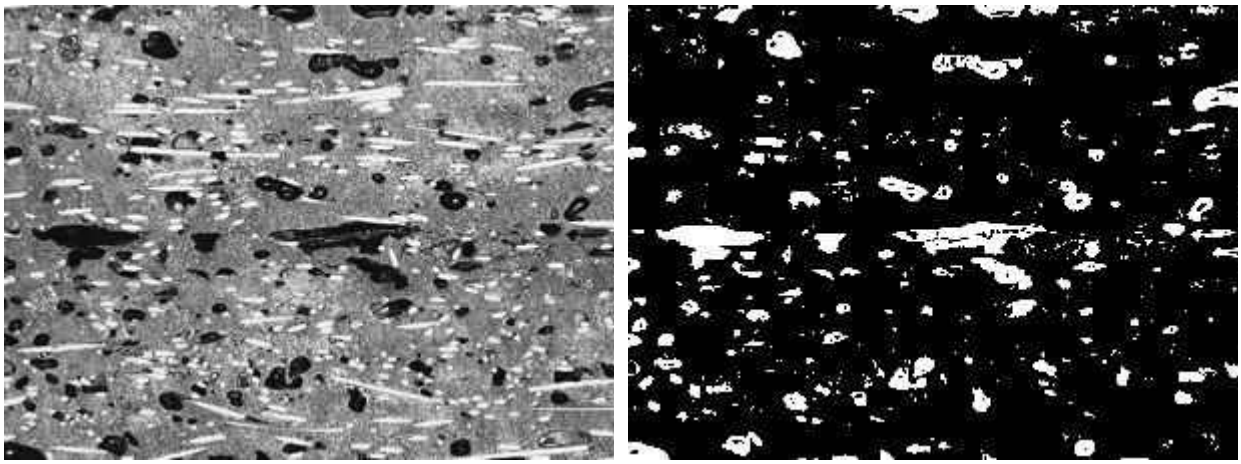

a. b.

Figure 32:Polished cross section micrograph captured from optical microscope (a) and analyzed image showing voids in white (b).

The micrographs clearly show that the void content decreases upon heating/annealing at 200C with the application of pressure. It is noticeable from the results (Table 5) that there is no much decrease in void content when the samples are annealed at 170 C. But when comparing the micrograph of pristine sample (Fig 33) and sample annealed with compaction at 200C (Fig 35), the void content of the pristine samples tends to decrease from 37.71% to 3.40% (Table 5) as the temperature of the reaches 200 C which is closer to the melting temperature 206 C. Since voids act as crack initiation in a sample, the decrease in the void content will result in increase of mechanical properties such as strength and modulus of the composite (Table 2).

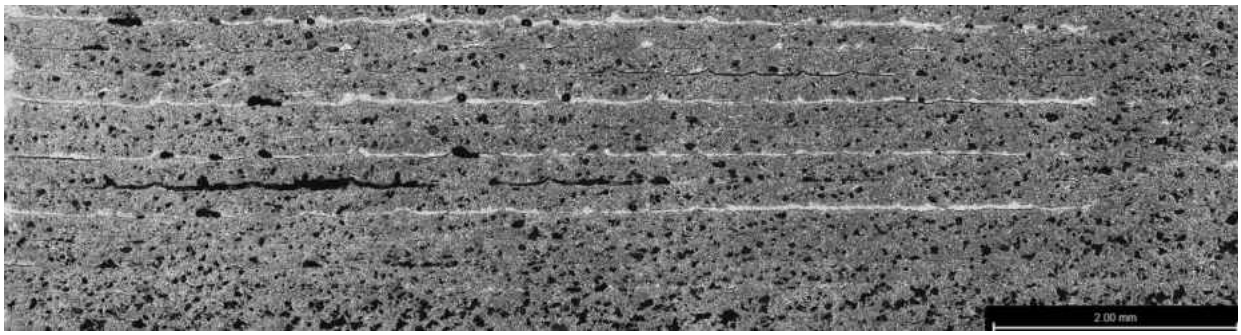

PS00

Figure 33: Micrograph of polished cross section of pristine samples with 0-degree print orientation

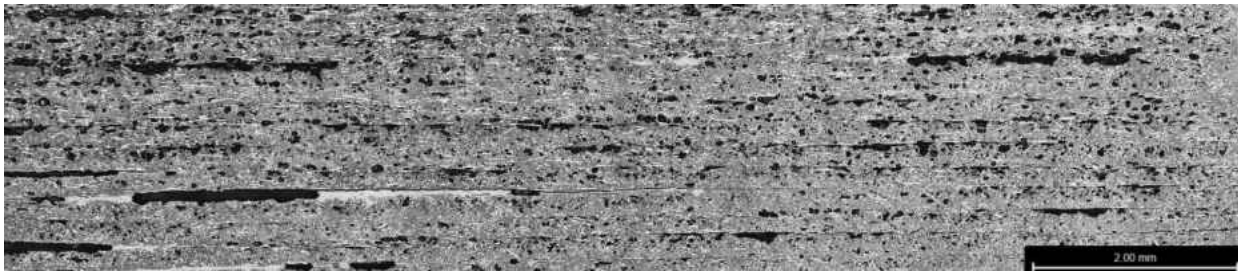

170AC00

Figure 34:Micrograph of polished cross section of samples annealed at 170 with 0-degree print orientation

200AC00

Figure 35:Micrograph of polished cross section of samples annealed and compacted at 200 C with 0-degree print orientation

3.7 Volume Fraction of Voids

The volume fraction of voids for the sample PS00 correspond to Fig33, 170AN00 mentioned in the table corresponds to the micrograph in the Fig 34. Similarly, the 200AC00 correspond to Fig 35. It can be observed that the void content tends to be relatively lesser for compacted specimens compared to the as printed/pristine and the annealed specimens. This shows that the compaction, which was previously reported, resulted in decrease of space between individual beads and reduced void content.

Table 5:Volume fraction of voids

Sample	Volume fraction of voids
Pristine (PS00)	37.71
Annealed at 170 C (170AN00)	23.08
Compacted at 200C (200AC00)	3.40

3.8 Fiber Orientation

The fiber orientation from the micrographs of the polished surfaces is calculated from the equations mentioned in section 2.5.1.

For pristine sample: PS00B,

$$A_{ij} = \begin{bmatrix} 0.610 & 0.257 \\ 0.257 & 0.390 \end{bmatrix}$$

For sample annealed at 170° C: 170AN00B,

$$A_{ij} = \begin{bmatrix} 0.547 & 0.244 \\ 0.244 & 0.453 \end{bmatrix}$$

For sample annealed and compacted at 200° C: 200AC00B,

$$A_{ij} = \begin{bmatrix} 0.619 & 0.265 \\ 0.265 & 0.381 \end{bmatrix}$$

It is observed that the fiber alignment is retained even when the samples are heat treated with compaction at 200C.

CHAPTER 4

CONCLUSION

Nylon-glass fiber composites with desired shape and dimensions were obtained from 3D printing. However, these samples did not exhibit higher strength and modulus due to weak bonding between individual deposited beads. Post-treatment such as annealing resulted in an increase in resin flow within the sample which in turn resulted in change in crystalline structure. Further application of pressure at a temperature relatively closer to the melting temperature resulted in an increase in the tensile strength and modulus.

Macroscopic deformation in the sample was investigated by determining the degree of compaction. A compaction strain of 20% was achieved when the samples were compacted at 200C. The reason for this change in degree of compaction can be explained by the microscopic analysis. A reduction in the void content of pristine samples from 37.71% for pristine to 3.40% is achieved by annealing with compaction at 200C.

The DSC results proved clearly that both modulus and strength of glass fiber composites increase with increase in crystallinity. An increase in degree of crystallinity was observed for samples compacted at 200C. It can be concluded that annealing of short fiber reinforced nylon at 200C with compaction pressure of 80psi exhibit improved strength and modulus without changing its original shape.

REFERENCES

[1] O. Ishai and I. Daniel, "*Engineering Mechanics of Composite Materials*," in *Engineering Mechanics of Composite Materials*, 2nd Edition., New York: Oxford Press, p. 37.

[2] B. Astrom, *"Manufacturing of Polymer Composites,"* in Manufacturing of Polymer Composites, 1st Edition., Champan and Hall, p. 301.

[3] T. Hofstätter, D. B. Pedersen, G. Tosello, and H. N. Hansen, *"State-of-the-art of fiber-reinforced polymers in additive manufacturing technologies,"* Journal of Reinforced Plastics and Composites, vol. 36, no. 15, pp. 1061–1073, Aug. 2017, doi: 10.1177/0731684417695648.

[4] H. Prüß and T. Vietor, *"Design for Fiber-Reinforced Additive Manufacturing," J. Mech. Des, vol. 137, no. 11, Nov. 2015, doi: 10.1115/1.4030993.*

[5] C. Koch, L. Van Hulle, and N. Rudolph, *"Investigation of mechanical anisotropy of the fused filament fabrication process via customized tool path generation,"* Additive Manufacturing, vol. 16, pp. 138–145, Aug. 2017, doi: 10.1016/j.addma.2017.06.003.

[6] H. Li, T. Wang, Q. Li, Z. Yu, and N. Wang, *"A quantitative investigation of distortion of polylactic acid/PLA) part in FDM from the point of interface residual stress," Int J Adv Manuf Technol, vol. 94, no. 1, pp. 381–395, Jan. 2018, doi: 10.1007/s00170-017-0820-*1.

[7] T. D. McLouth, J. V. Severino, P. M. Adams, D. N. Patel, and R. J. Zaldivar, *"The impact of print orientation and raster pattern on fracture toughness in additively manufactured ABS,"* Additive Manufacturing, vol. 18, pp. 103–109, Dec. 2017, doi: 10.1016/j.addma.2017.09.003.

[8] H. Unal, A. Mimaroglu, *"Influence of Filler Addition on the Mechanical Properties of Nylon-6 Polymer".*

[9] Suresh Chandra Kuchipudi Minnesota State University, Mankato "*The Effects of Fiber Orientation and Volume Fraction of Fiber on Mechanical Properties of Additively Manufactured Composite Material".*

[10] Weihong Zhong, Fan Li, Zuoguang Zhang, Lulu Song, Zhimin Li, "*Short fiber reinforced composites for fused deposition modeling*".

[11] Easir Arafat Papon, Anwarul Haque, ***"****Tensile properties, void contents, dispersion and fracture behaviour of 3D printed carbon nanofiber reinforced composites****".***

[12] Nahal Aliheidari, Rajasekhar Tripuraneni, Amir Ameli, SivaNadimpalli, *"Fracture resistance measurement of fused deposition modeling 3D printed polymers".*

[13] J. Justo, L. Távara, L. García-Guzmán, F. París, *"Characterization of 3D printed long fibre reinforced composites".*

[14] Ramirez, M., et al. *"Computational Damage Modeling of Additively Manufactured Short Fiber Composite Material."* Science in the Age of Experience (2018).

[15] Qingyu Meng Yizhuo Gu, Liang Luo, Shaokai Wang, Min Li, Zuoguang Zhang, "*Annealing effect on crystalline structure and mechanical properties in long glass fiber reinforced polyamide 66****".***

[16] Marcus Ivey,Garrett W. Melenka,Jason. P. Carey &Cagri Ayranc, *"Characterizing short-fiber-reinforced composites produced using additive manufacturing".*

[17] Sunil Bhandari, Roberto A.Lopez-Anido, Douglas J.Gardner, ***"****Enhancing the interlayer tensile strength of 3D printed short carbon fiber reinforced PETG and PLA composites via annealing****".***

[18] Y. Saito, F. Fernandez, D.A. Tortorelli, W.S. Compel, J.P. Lewicki, J. Lambros, "*Experimental Validation of an Additively Manufactured Stiffness-Optimized Short-Fiber Reinforced Composite Clevis Joint*".

[19] https://www.dynamism.com/xstrand.html?

[20] Anthony G. Tantillo, Rochester Institute of Technology, *"Annealing of Fused Filament Fabricated Nylon 6 with Elevated Annealing of Fused Filament Fabricated Nylon 6 with Elevated Isostatic Pressure".*

[21] Jianjum Zhang, Guazing Lu, *"Dynamic tensile behavior of re-entrant honeyc`ombs".*

[22] Vinod Srinivasa; Vinay Shivakumar; Vinay Nayaka; Sunil Jagadeeshaiaih; Murali Seethram; Raghavendra Shenoy; Abdelhakim Nafidi, *"Fracture Morphology on carbon fiber reinforced plastic composite laminate".*

[23] CélineVicard Olivier De Almeida, Arthur Cantarel, Gérard Bernhart, *"Experimental study of polymerization and crystallization kinetics of polyamide 6 obtained by anionic ring opening polymerization of ε-caprolactam***".**

[24] Yash P. Khanna, "*Overview of Transition Phenomenon in Nylon 6"*, Morristown, Research and Technology, Allied-Signal, Inc., New Jersey 07962.

[25] L. Penel-Pierron, C. Depecker, R. Séguéla, J.-M. Lefebvre "*Structural and Mechanical Behavior of Nylon 6 Films Part I. Identification and Stability of the Crystalline Phases*".

[26] N. S. Murthy and R. G. Bray Research and Technology, AlliedSignal Inc., PO Box 10.21, Morristown, NJ 07962, USA and S. T. Correale and R. A. F. Moore Fibers Division, AlliedSignal Inc., PO Box 31, Petersburg, VA 23804, USA, *"Drawing and annealing of nylon-6 fibres: studies of crystal growth, orientation of amorphous and crystalline domains and their influence on properties"*

[27] T. d. Bessell,, D. Hull, J. B. Shortall, *"The effect of polymerization conditions and crystallinity on the mechanical properties and fracture of spherulitic nylon 6",* Department of Metallurgy and Materials Science, University of Liverpool, UK.

VITA

Pushpashree Jain Ajith Kumar Jain

Department of Mechanical and Aerospace Engineering

Old Dominion University

Norfolk, VA 23529

Education

Master of Science in Mechanical Engineering. Department of Mechanical and Aerospace Engineering. Old Dominion University, Norfolk, VA-23529. December 2020.

Bachelor of Engineering in Aeronautical Engineering. Department of Aeronautical Engineering. MVJ College of Engineering. Visvesvaraya Technological University, India. June 2017.